Available online at www.sciencedirect.com
ScienceDirect
Journal of Power Sources 174 (2007) 1212–1217
JOURNAL OF POWER SOURCES
www.elsevier.com/locate/jpowsour

Short communication

Nanosized $LiM_YMn_{2-Y}O_4$ (M = Cr, Co and Ni) spinels synthesized by a sucrose-aided combustion method Structural characterization and electrochemical properties

J.M. Amarilla [a,*], R.M. Rojas [a], F. Pico [a], L. Pascual [a], K. Petrov [b], D. Kovacheva [b], M.G. Lazarraga [a], I. Lejona [a], J.M. Rojo [a]

[a] *Instituto de Ciencia de Materiales de Madrid, CSIC, Cantoblanco, 28049 Madrid, Spain*
[b] *Institute of General and Inorganic Chemistry, Bulgarian Academy of Sciences, 1113 Sofia, Bulgaria*

Available online 23 June 2007

Abstract

Spinels of composition $LiM_YMn_{2-Y}O_4$, M = Cr^{3+}, Co^{3+}, or Ni^{2+}, $Y = 0.1$ and 1 for the Cr and Co dopants, $Y = 0.05$ and 0.5 for the Ni sample, have been synthesized by a sucrose-aided combustion method. The samples as prepared require of an additional thermal treatment at 700 °C, 1 h to get stoichiometric single-phase spinels. The samples consist of aggregated particles of small size (45–50 nm) as deduced from transmission electron microscopy and X-ray powder diffraction. The electrochemical behaviour of the six spinels as cathodes in lithium cells has been analysed at 5 and 4 V under high current, 1 C rate. At 5 V the discharge capacity of $LiNi_{0.5}Mn_{1.5}O_4$ is higher than the one shown by $LiCrMnO_4$ and $LiCoMnO_4$, and it shows an elevated cyclability, i.e. capacity retention of 85.3% after 100 cycles. At 4 V the discharge capacity is similar for $LiNi_{0.05}Mn_{1.95}O_4$, $LiCr_{0.1}Mn_{1.9}O_4$ and $LiCo_{0.1}Mn_{1.9}O_4$, and all the three spinels show similar and very high cyclability, i.e. capacity retention >90% after 100 cycles. The spinels preserve their starting capacity up to currents as high as 2 C rate. The nanometric size of the samples explains the high rate capability of the synthesized spinels.

Keywords: Lithium battery; Cathode material; Spinel; 4 V and 5 V electrodes; $LiMn_2O_4$; $LiNi_{0.5}Mn_{1.5}O_4$

1. Introduction

Recent trends in Li-ion batteries are focused on the development of active electrode materials with high energy density and elevated rate capability [1–4]. Regarding the cathode materials, $LiMn_2O_4$-based materials with general formula $LiM_YMn_{2-Y}O_4$, are promising candidates because their high voltage, low cost and satisfactory environmental friendliness [5–7]. In addition, notable improvement of the 4 V reversible capacity has been achieved by doping with small amounts ($Y \leq 0.2$) of several ions, i.e. by substituting a part of Mn by other metal cations [8,9]. On the other hand, doping also allows increasing the working voltage from 4 to 5 V, and consequently the energy density [10,11]. This effect is particularly significant for high dopant content, e.g. $Y = 1$ for M^{3+} dopants or $Y = 0.5$ for M^{2+} one. Since, in $LiMn_2O_4$-based electrodes the Li^+ diffusion coefficient is low [12], the most realistic option to get an elevated rate capability is to use nanosized materials that if are properly doped both objectives, elevated rate capability and high energy density can be attained.

We have recently developed a new, cheap and rapid sucrose-aided combustion method, which is adequate for preparing homogeneous nanosized materials [11,13]. This method is based on the reaction of the preset amounts of Li, Mn, and M nitrates, which act as oxidants, and sucrose, which operates as fuel. Aimed to synthesize $LiMn_2O_4$-based spinels with high rate capability, i.e. with small particle size, we have undertaken the synthesis of several low-doped $LiM_YMn_{2-Y}O_4$ (M = Cr, Co, $Y = 0.1$ and Ni, $Y = 0.05$) and high-doped $LiM_YMn_{2-Y}O_4$ (M = Cr, Co, $Y = 1$; Ni, $Y = 0.5$) spinels by this combustion method. All the synthesized samples have been structural and morphologically characterized, and with these samples cathodes have been processed. The discharge capacity and the cycling behaviour at 5 and 4 V have been studied. We have also assessed the rate capability in a broad current range, from C/2 to 6 C.

* Corresponding author.
E-mail address: amarilla@icmm.csic.es (J.M. Amarilla).

0378-7753/$ – see front matter © 2007 Elsevier B.V. All rights reserved.
doi:10.1016/j.jpowsour.2007.06.056

2. Experimental

Samples of composition $LiCr_{0.1}Mn_{1.9}O_4$, $LiCo_{0.1}Mn_{1.9}O_4$, $LiNi_{0.05}Mn_{1.95}O_4$, hereafter referred as LD-spinels, and $LiCrMnO_4$, $LiCoMnO_4$, and $LiNi_{0.5}Mn_{1.5}O_4$, named as HD-spinels, were obtained following the procedure reported elsewhere [13]. Preset stoichiometric amounts of reagent grade Li(I), Mn(II), Cr(III), Co(II) or Ni(II) nitrate were dissolved in the minimum amount of distilled water, and the fuel (sucrose) was then added to the solution. After slow evaporation at 120 °C a voluminous foamy mass was obtained. Then it spontaneously burned and transformed into a black sponge-like fluffy product. The as-prepared samples were additionally heated at 700 °C, 1 h in still air at 2 °C min^{-1} heating/cooling rate. X-ray diffraction patterns (XRD) were recorded at room temperature in a D8 Bruker diffractometer, with CuKα radiation. The patterns were obtained in the step scanning mode at 0.02° (2θ) and 1 s $step^{-1}$ counting time, within the range $15° \leq 2\theta \leq 80°$. Lattice parameter was refined with the CELREF program [14]. The average crystallite size, D, was calculated from the full width at half maximum (FWHM) of several diffraction lines by applying the Scherrer equation $D = \lambda/\beta \cos\theta$; where λ is the wavelength of the X-rays, θ is the diffraction angle, and $\beta = \sqrt{(\beta_{m-}^2 \beta_s^2)}$ is the corrected FWHM, where β_m is the observed FWHM of the experimental diffraction peaks, and β_s is the FWHM of the diffraction peaks of $LiNi_{0.5}Mn_{1.5}O_4$ previously heated at 1000 °C, used as standard.

Transmission electron (TEM) micrographs and electron diffraction (ED) patterns were taken in a JEOL 2000 FX microscope operating at an acceleration voltage of 200 kV. The samples were dispersed in *n*-butyl alcohol. Drops of the dispersion were transferred to a holey carbon-coated copper grid.

Charge/discharge galvanostatic experiments were carried out with an Arbin battery tester system (BT2043). The voltage range was 3.4–5.2 V. The temperature was kept at 25.0 ± 0.2 °C. The experiments were carried out at 0.5 C rate in charge and at 1 C rate in discharge. The positive electrodes were composites, which were processed from the already mentioned spinels (≈20 mg or 72 wt.%), MMM Super P carbon black (17 wt.%) and PVDF (11 wt.%) These contents were chosen in accordance with those reported elsewhere [15]. The *N*-methylpyrrolidinone (1 mL g^{-1} of PVDF) was added to the mixture of the three components, and they were stirred overnight. The solvent was evaporated at 80 °C. Then cylindrical pellets (12 mm diameter and ≈0.2 mm thickness) of positive electrode were obtained after cold pressing at 370 MPa. The electrolyte, 1 M solution of $LiPF_6$ in ethylene carbonate and dimethyl carbonate as supplied by Merck, was impregnated into a separator Whatman BSF80 paper. The negative electrode was a lithium foil, which also operated as reference electrode. The two electrodes and the separator were assembled in Swagelock®-type cells, within a glove box in which the water content was below 1 ppm. Rate capability testing was performed by discharging the cells at rates ranging from 0.2 to 6 C and at 25.0 ± 0.2 °C. Charge rate was 0.5 C in all cases except for 0.2 C for which both charge and discharge processes were developed at 0.2 C rate.

3. Results and discussion

3.1. Structural and morphological characterization

The XRD patterns of the samples with composition $LiM_YMn_{2-Y}O_4$ (M = Co, Y = 0.1 and 1) are shown in Fig. 1a–d. The patterns have been recorded on the samples as prepared, and on these samples after heating at 700 °C, 1 h. This temperature has been chosen in accordance with results obtained on some others as-prepared spinels [16]. In all patterns we see the characteristic diffractions peaks of the spinel-type structure. In the pattern of the as-prepared Co-sample at Y = 0.1 (Fig. 1a) we also see some extra peaks ascribed to Mn_3O_4 (asterisks marked). This impurity is always present in all the as-prepared samples with low dopant content, i.e. $LiCr_{0.1}Mn_{1.9}O_4$ and $LiNi_{0.05}Mn_{1.95}O_4$ (not shown). After heating at 700 °C the Mn_3O_4 peaks disappear from the XRD patterns, and the patterns of the 700 °C-heated samples only show the typical peaks of the spinel-type structure (see Fig. 1b for the $LiCo_{0.1}Mn_{1.9}O_4$ sample). The XRD pattern of the as-prepared Y = 1 Co-doped sample only shows the spinel peaks (Fig. 1c). In it we clearly see the (2 2 0) peak at $2\theta \approx 31°$, which is associated with the presence of heavy cations in tetrahedral 8a sites of the spinel-type structure (S.G. Fd3m). Rietveld refinement revealed that the occupancy of the tetrahedral 8a sites by heavy atoms is 0.32 for the as-prepared sample. After heating at 700 °C (Fig. 1d) the intensity of the mentioned (2 2 0) peak decreases, and the occupancy by heavy atoms drops to 0.13. For the 700 °C-heated $LiCrMnO_4$ and $LiNi_{0.5}Mn_{1.5}O_4$

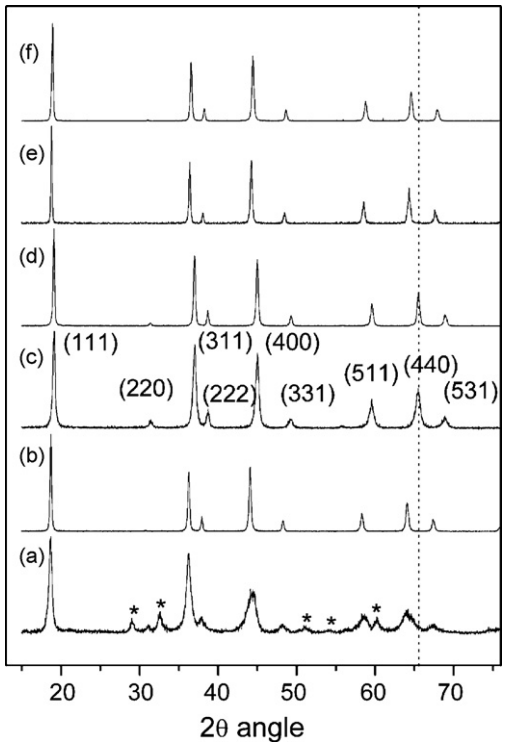

Fig. 1. X-ray powder diffraction patterns recorded for the $LiCo_YMn_{2-Y}O_4$ spinels: (a) Y = 0.1 as prepared; (b) Y = 0.1 heated at 700 °C, 1 h; (c) Y = 1 as-prepared, (d) Y = 1 heated at 700 °C, 1 h; (e) 700 °C-heated $LiCrMnO_4$; (f) 700 °C-heated $LiNi_{0.5}Mn_{1.5}O_4$ (*Mn_3O_4).

Table 1
Cubic lattice parameter and crystallite size determined for the 700 °C-heated $LiM_YMn_{2-Y}O_4$ spinels synthesized by the sucrose-aided combustion procedure

Composition	Lattice parameter a (Å)	Crystallite size* (nm)
$LiCr_{0.1}Mn_{1.9}O_4$	8.2413(5)	48
$LiCrMnO_4$	8.2021(6)	50
$LiCo_{0.1}Mn_{1.9}O_4$	8.229(2)	45
$LiCoMnO_4$	8.067(1)	45
$LiNi_{0.05}Mn_{1.95}O_4$	8.2426(5)	47
$LiNi_{0.5}Mn_{1.5}O_4$	8.1782(4)	47

* Determined from the Scherrer equation.

spinels the (2 2 0) peak is not observed in the corresponding XRD patterns (Fig. 1e and f). On the other hand, the thermal treatment of all samples gives rise to a narrowing of the XRD peaks (see Fig. 1a–d as example). The crystallite size increases from ≈20 nm for the as-prepared samples, to ≈50 nm for the 700 °C-heated samples. It is also worth to mention that the pattern of the 700 °C-heated $LiNi_{0.5}Mn_{1.5}O_4$ does not show any peaks ascribable to NiO or $Li_xNi_{1-x}O$ (Fig. 1f), impurities generally observed when the sample is synthesized by other soft-chemistry methods [17–19].

In Table 1, the lattice parameter for the 700 °C-heated $LiM_YMn_{2-Y}O_4$ spinels is given. All the lattice parameters are smaller than the one reported for $LiMn_2O_4$, $a = 8.24762(16)$ Å [35-0782 JCPDS file]. For the Cr- and Co-doped spinels it can be accounted for having in mind the smaller ionic radii, $^{VI}Cr^{3+}$ (0.615 Å) and $^{VI}Co^{3+}$ (0.545 Å), compared to the ionic radius of $^{VI}Mn^{3+}$ (0.645 Å) [20] to which the former two cations are substituted for. Based on this, the Cr and Co HD-spinels have smaller lattice parameter than the LD-spinels. Regarding the Ni-doped spinel, and in spite of the ionic radius of $^{VI}Ni^{2+}$ (0.69 Å), the simultaneous formation of $^{VI}Mn^{4+}$ (0.53 Å) on substituting Mn^{3+} by Ni^{2+} to keep the electroneutrality of the compound, accounts for the shrinkage of the lattice.

TEM micrograph and ED pattern of the 700 °C-heated $LiCr_{0.1}Mn_{1.9}O_4$ are shown in Fig. 2. We see aggregated individual particles rather uniform in size. The particle size distribution is shown in the joined histogram fitted to a Gaussian curve. The average particle size is 45 nm, which agrees with the crystallite size deduced from XRD (48 nm, Table 1). It is so because the particles are single crystals, as evidenced by the ED pattern, which exhibits a typical spinel diffraction pattern in the zone axis [0 1 1]. Moreover, it is worth to note that the particle size (or crystallite size) of the 700 °C-heated Cr, Co, and Ni spinels is similar, ≈50 nm. Then it follows that the sugar-aided combustion procedure developed by us is a powerful synthesis method that allows preparation of single-phase $LiMn_2O_4$-based spinels with similar nanometric particle size, and of any chemical composition.

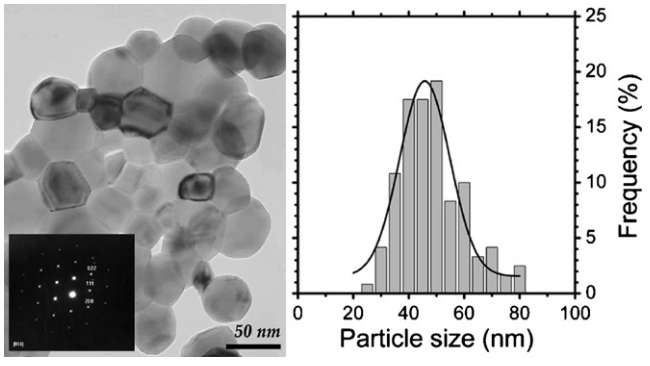

Fig. 2. TEM image, ED pattern, and particle size histogram of the 700 °C-heated $LiCr_{0.1}Mn_{1.9}O_4$ spinel.

3.2. Electrochemical behaviour

Electrochemical studies were performed on the 700 °C-heated $LiM_YMn_{2-Y}O_4$ spinels. The charge/discharge curves obtained in the 5 and 4 V potential regions for the HD- and LD-spinels, respectively, are shown in Fig. 3. In the 5 V region the discharge curve recorded for the $LiNi_{0.5}Mn_{1.5}O_4$ sample shows two plateaus at 4.59 and 4.66 V that have been associated with the $Ni^{2+} \Leftrightarrow Ni^{3+}$ and $Ni^{3+} \Leftrightarrow Ni^{4+}$ couples, respectively [21]. The discharge curves recorded for the $LiCrMnO_4$ and $LiCoMnO_4$ spinels are similar, and more sloping than the one recorded for the Ni sample. For the two samples, the charge capacity is significantly higher than the discharge one. This result points to some degradation of the electrolyte due to the high potentials attained at the end of the charge stage. In the 4 V region the charge/discharge curves of the $LiCr_{0.1}Mn_{1.9}O_4$, $LiCo_{0.1}Mn_{1.9}O_4$ and $LiNi_{0.05}Mn_{1.95}O_4$ spinels have a similar shape, showing the usual two plateaus developed at 4.1 and 4.2 V in charge, and 3.8 and 4 V in discharge (Fig. 3). Moreover, the charge/discharge capacities are similar indicating that in this potential region no noticeably degradation of the electrolyte during charge takes place.

The values of the first discharge capacity, Q, are summarized in Table 2. In the 5 V region and, according to the electrochem-

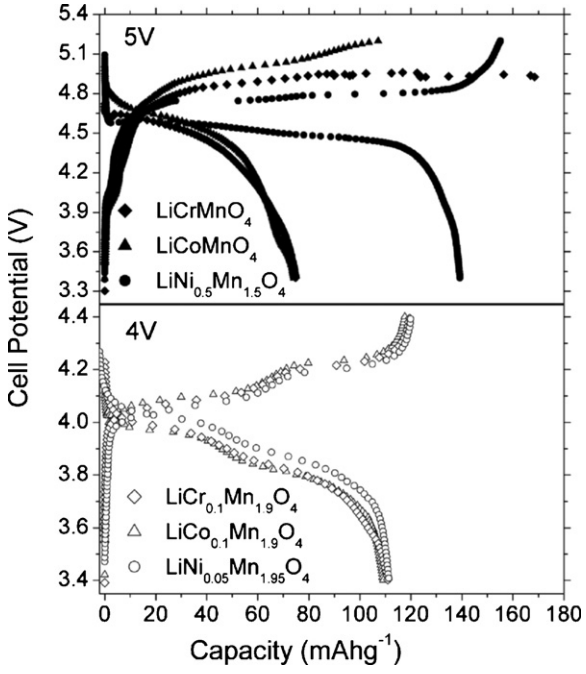

Fig. 3. Charge/discharge curves of the 700 °C-heated $LiM_YMn_{2-Y}O_4$ spinels in the 5 and 4 V regions at 0.5 C charge and 1 C discharge rates.

Table 2
Discharge capacity (Q), capacity loss by cycle, and capacity retention of the 700 °C-heated $LiM_YMn_{2-Y}O_4$ spinels synthesized by the sucrose-aided combustion procedure

Composition	Q (mA h g^{-1}) 5 V* or 4 V+	Capacity loss (mA h g^{-1} cycle^{-1})	Capacity retention after 100 cycles (%)
$LiCrMnO_4$	74.4*	−9.6	0
$LiCoMnO_4$	74.2*	−0.56	25
$LiNi_{0.5}Mn_{1.5}O_4$	139.3*	−0.18	85.3
$LiCr_{0.1}Mn_{1.9}O_4$	111.0+	−0.095	91.5
$LiCo_{0.1}Mn_{1.9}O_4$	109.2+	−0.026	97.6
$LiNi_{0.05}Mn_{1.95}O_4$	113.3+	−0.055	95.1

ical reactions:

$$Li^+M^{3+}Mn^{4+}O_4 \rightarrow M^{4+}Mn^{4+}O_4 + Li^+ + e^- (M^{3+} = Cr^{3+}, Co^{3+})$$

$$Li^+Ni_{0.5}{}^{2+}Mn_{1.5}{}^{4+}O_4 \rightarrow Ni_{0.5}{}^{4+}Mn_{1.5}{}^{4+}O_4 + Li^+ + e^-$$

It should be expected that all the three HD-spinels would show similar capacity, $Q_{theor} \approx 147$ mA h g^{-1}. For the $LiNi_{0.5}Mn_{1.5}O_4$, and in spite of the high discharge current chosen, 1 C rate, the capacity is 139.3 mA h g^{-1}, which is close to the theoretical one, 146.7 mA h g^{-1}. This experimental capacity is higher than the one reported for a nanometric spinel of the same composition [22]. These results suggest that the $LiNi_{0.5}Mn_{1.5}O_4$ synthesized by us has a high rate-capability. However, for $LiCrMnO_4$ and $LiCoMnO_4$ the capacities measured, 74.4 and 74.2 mA h g^{-1}, respectively, are anomalously small, nearly half their theoretical values. The low experimental capacity measured in $LiCoMnO_4$ can be accounted for considering: (i) the charge process done up to 5.2 V was not sufficient to complete the extraction of Li^+ (Fig. 3) and (ii) the presence of some heavy cations in the tetrahedral 8a sites of the spinel structure, as shown by XRD (Fig. 1d). This occupancy makes the 8a sites no longer accessible to the Li ions, and consequently is not possible to extract 1Li^+ per formula, as it is assumed in the electrochemical reaction. Regarding the $LiCrMnO_4$ spinel, some degradation of the electrolyte takes place along the charge process (Fig. 3). It hampers to reach a charge potential higher than 4.9 V, even though several cells were measured. It seems that this particular sample promote severe decomposition of the electrolyte.

At 4 V, the discharge capacity is practically the same for the three LD-spinels (Table 2). It is worth to remark that the values are very close to the theoretical capacity $Q_{theor} \approx 133$ mA h g^{-1} deduced from the electrochemical reactions:

$$LiM_{0.1}{}^{3+}Mn^{3+}{}_{0.9}Mn^{4+}O_4 \rightarrow Li_{0.1}M_{0.1}{}^{3+}Mn_{1.9}{}^{4+}O_4 + 0.9(Li + e)$$

$$LiNi_{0.05}{}^{2+}Mn^{3+}{}_{0.9}Mn_{1.05}{}^{4+}O_4 \rightarrow Li_{0.1}Ni_{0.05}{}^{2+}Mn_{1.95}{}^{4+}O_4 + 0.9(Li + e)$$

The likeness between capacities is coherent given that Mn^{3+} is the electrochemically active cation in the 4 V region, and the amount of Mn^{3+} is the same in the three samples.

The long-term cyclability of the HD- and LD-spinels at 5 and 4 V, respectively, has also been examined (Fig. 4). From the inspection of the curves, it follows that at 5 V, the cycling behaviour strongly depends on the dopant cations. For $LiNi_{0.5}Mn_{1.5}O_4$, the discharge capacity decreases linearly on cycling. The slope of the straight line is small, −0.18 mA h g^{-1} cycle^{-1}, being the capacity retention of 85.3% after 100 cycles. This capacity retention shows that $LiNi_{0.5}Mn_{1.5}O_4$ has a good cyclability. It is much better than the one shown by the two other HD-$LiMMnO_4$ (M = Cr, Co) spinels. For these latter samples, Q also decreases linearly on cycling. However, the slopes determined for $LiCoMnO_4$, −0.56 mA h g^{-1} cycle^{-1}, and for $LiCrMnO_4$, −9.6 mA h g^{-1} cycle^{-1}, are significantly higher in absolute value, than the one determined for $LiNi_{0.5}Mn_{1.5}O_4$.

The capacity of $LiCrMnO_4$ becomes zero after only 10 cycles (Fig. 4). To account for this dramatic drop in capacity, the XRD pattern of the 50-cycled $LiCrMnO_4$ was recorded. It shows a sensible decrease in the intensity ratio of the (1 1 1)/(4 0 0) and (3 1 1)/(4 0 0) diffraction peaks compared to the one observed for the pristine material (Fig. 5a). Moreover, the lattice parameter shrinks, from 8.2021(6) Å determined for the pristine material (Table 1), to 8.191(1) Å for the cycled sample. These variations

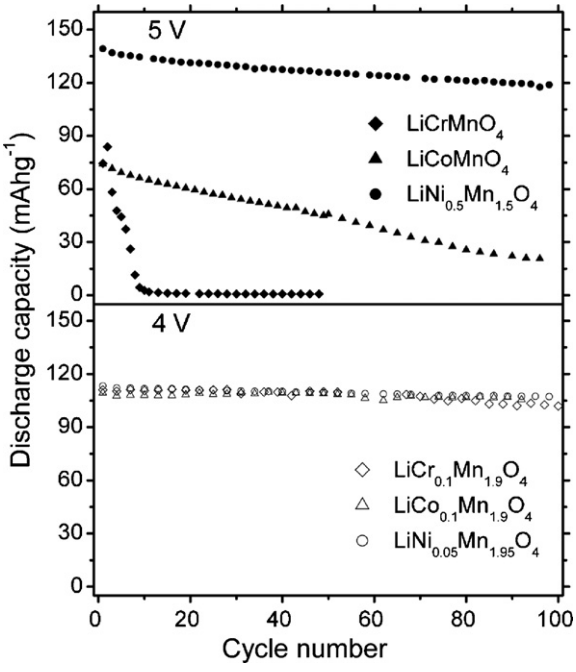

Fig. 4. Cycling performance in the 5 and 4 V potential region of the 700 °C-heated $LiM_YMn_{2-Y}O_4$ spinels at 0.5 C charge and 1 C discharge rates.

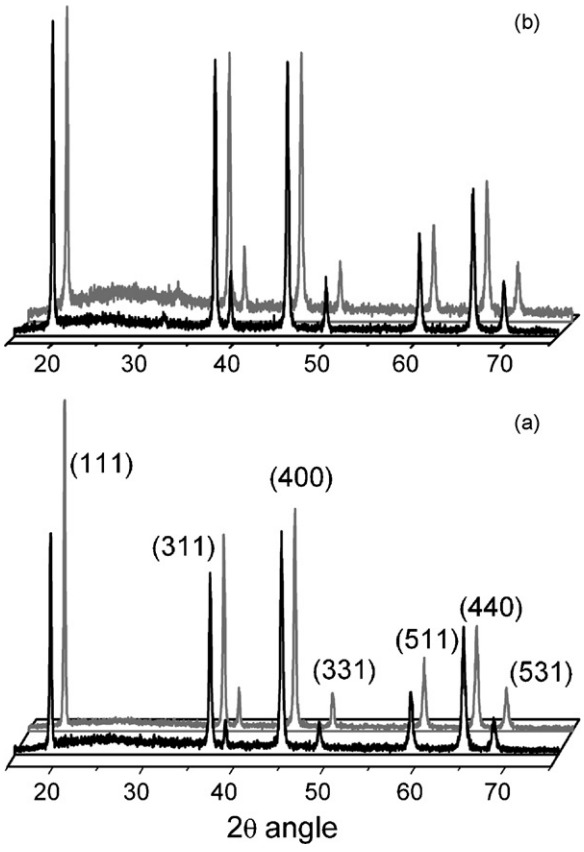

Fig. 5. XRD patterns of the 700 °C-heated $LiMMnO_4$ spinels: (a) M = Cr; (b) M = Co. The patterns were recorded on the cathode composites before (grey line) and after (black line) cycling in the 5 V region.

indicate that some structural modifications have taken place, and it could explain the observed capacity fade that $LiCrMnO_4$ undergone upon cycling, as has been proposed by Sigala et al. from neutron diffraction studies [23].

The cyclability of the $LiCoMnO_4$ is intermediate between those shown by $LiNi_{0.5}Mn_{1.5}O_4$ and $LiCrMnO_4$ (Fig. 4 and Table 2). We have analysed the XRD pattern of the 100-cycled $LiCoMnO_4$, but differences neither in intensity nor in position of the peaks between the pattern of the cycled sample and that of the pristine one were observed (Fig. 5b). The lattice parameter of the sample after 100 cycles, $a = 8.064(1)$ Å, is practically identical to the one determined for the pristine material, $a = 8.067(1)$ Å. This result indicates that the capacity loss is not justifiable in terms of structural changes of the $LiCoMnO_4$ spinel. Moreover, the coulombic efficiency, $Q_{discharge}/Q_{charge}$ ratio, is ≈89% by cycle, indicating that some degradation of the electrolyte takes place every charge step, and it could be at the origin of the loss of capacity on cycling.

In the 4 V region, the long-term cyclability of the LD-spinels $LiCr_{0.1}Mn_{1.9}O_4$, $LiCo_{0.1}Mn_{1.9}O_4$, and $LiNi_{0.05}Mn_{1.95}O_4$ is similar (Fig. 4). In these samples, a very small and near linear decrease of capacity is observed, $|slope| \leq 0.1$ mA h g^{-1} $cycle^{-1}$. The retention capacity is very high, >90% after 100 cycles (Table 2), and it leads us to conclude that the cyclability of the LD-spinels is very elevated, >99.9% by cycle; much better than the one shown by the

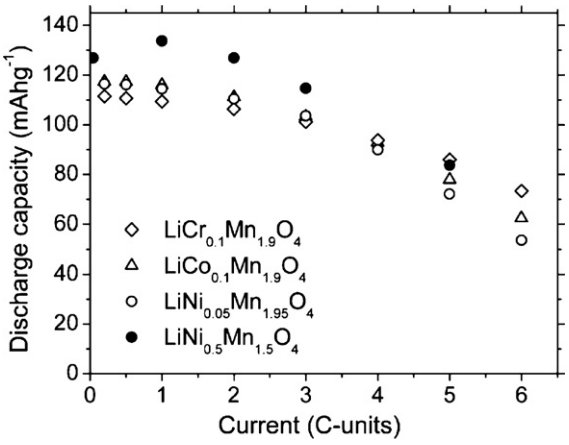

Fig. 6. Variation of the discharge capacity vs. current for several 700 °C-heated $LiM_YMn_{2-Y}O_4$ spinels. (C ≈3 mA and the potential ranges were: 3.4–5.2 V for $LiNi_{0.5}Mn_{1.5}O_4$ and 3.1–4.4 V for $LiCr_{0.1}Mn_{1.9}O_4$, $LiCo_{0.1}Mn_{1.9}O_4$, and $LiNi_{0.05}Mn_{1.95}O_4$).

HD-spinels. The XRD patterns of the 4 V cycled samples show that the starting cubic spinels structure remains without any modification after 100 cycles. This is an expected result, considering the very good cyclability of the samples. Moreover, the $E_{cut\text{-}off}$ potentials required for the charge of the LD-spinels, 4.4 V, avoids the electrolyte degradation; the coulombic efficiency is >99.5% by cycle.

The rate capability of the samples has been determined evaluating the variation of the discharge capacity versus current (Fig. 6). All the samples analysed show similar behaviour, and two regions can be distinguished: (i) one region up to 2 C rate, in which capacity remains almost constant and (ii) another region above 2 C rate, in which the capacity decreases linearly on increasing the current due to kinetic limitations. The likeness in behaviour shows that the rate capability does not depend on the dopant cations. The similitude of the rate capability can be related with the comparable particle size of the samples (Table 1). It is worth to note that the analysed spinels exhibit a remarkable rate capability that can be attributed to their nanometric particle size.

4. Conclusions

The sucrose-aided combustion method is a rapid, cheap, powerful, and straightforward synthesis procedure that yields $LiM_YMn_{2-Y}O_4$ single-phase spinels, with different dopant cations (M = Cr, Co and Ni), and in a broad compositional range ($0 \leq Y \leq 1$). In all cases, the samples have nanometric particle size, ≈50 nm, as deduced from TEM and XRD. The HD-spinels are electrochemically active in the 5 V region and the LD-spinels in the 4 V region. For the former, the cyclability depends strongly on the dopant cation, while for the LD-spinels the cyclability is similar, i.e. does not depend on the dopant cation. The $LiNi_{0.5}Mn_{1.5}O_4$ as well as the three LD-$LiM_YMn_{2-Y}O_4$ exhibit an excellent electrochemical performance. The starting capacities are 139.3 mA h^{-1} g^{-1} and ≈110 mA h^{-1} g^{-1}, respectively. The cyclability is very high, with a capacity retention >85% after 100 cycles. These samples also show a high rate capability, the

capacity being nearly constant up to 2 C rate. These outstanding properties make the synthesized spinels suitable cathodes for high energy/high power rechargeable Li-ion batteries.

Acknowledgements

Financial support through the projects MAT 2005-01606 (MEC), GR/MAT/0426/2004 (CAM) and the joint project CSIC-Bulgarian Academy of Sciences no. 2004BG0010 is thankfully recognized.

References

[1] J.M. Tarascon, M. Armand, Nature 414 (2001) 359.
[2] M.S. Whittingham, Chem. Rev. 104 (2004) 4271.
[3] A.S. Aricó, P.G. Bruce, B. Scrosati, J.M. Tarascon, W. Van Schalkwijk, Nat. Mat. 4 (2005) 366.
[4] F.F.C. Bazito, R.M. Torresi, J. Braz. Chem. Soc. 17 (2006) 627.
[5] M.M. Thackeray, Prog. Solid State Chem. 25 (1997).
[6] G. Amatucci, J.M. Tarascon, J. Electrochem. Soc. 149 (2002) K31–K46.
[7] Y. Xia, M. Yoshio, in: Nazri, G. Pistoia (Eds.), Science and Technology of Lithium Batteries, Kluwer Academia Publishers, 2004 (Chapter 12).
[8] J.M. Tarascon, E. Wang, F.K. Shokoohi, W.R. McKinnon, J. Electrochem. Soc. 138 (1991) 2859.
[9] L. Guohua, H. Ikuta, T. Uchida, M. Wakihara, J. Electrochem. Soc. 143 (1996) 178.
[10] H. Kawai, M. Nagata, H. Kageyama, H. Tukamoto, A.R. West, Electrochim. Acta 45 (1999) 315.
[11] M.G. Lazarraga, L. Pascual, H. Gadjov, D. Kovacheva, K. Petrov, J.M. Amarilla, R.M. Rojas, M.A. Martín-Luengo, J.M. Rojo, J. Mater. Chem. 14 (2004) 1640.
[12] E. Deiss, D. Häringer, P. Novák, O. Hass, Electrochim. Acta 46 (2001) 4185.
[13] D. Kovacheva, H. Gadjov, K. Petrov, S. Mandal, M.G. Lazarraga, L. Pascual, J.M. Amarilla, R.M. Rojas, P. Herrero, J.M. Rojo, J. Mater. Chem. 12 (2002) 1184.
[14] J. Laugier, A. Filhol, CelRef, PC version CELREF program, ILL, Grenoble, Francia, 1991 (unpublished).
[15] M.G. Lazarraga, S. Mandal, J. Ibañez, J.M. Amarilla, J.M. Rojo, J. Power Sources 115 (2003) 315.
[16] L. Pascual, H. Gadjov, D. Kovacheva, K. Petrov, P. Herrero, J.M. Amarilla, R.M. Rojas, J.M. Rojo, J. Electrochem. Soc. 152 (2005) A301.
[17] Q. Zhong, A. Bonakdarpour, M. Zhang, Y. Gao, J.R. Dahn, J. Electrochem. Soc. 144 (1997) 205.
[18] T. Ohzuku, K. Ariyoshi, S. Yamamoto, J. Ceram. Soc. Jpn. 110 (2002) 501.
[19] R. Alcántara, M. Jaraba, P. Lavela, J.L. Tirado, Electrochim. Acta 47 (2002) 1829.
[20] R.D. Shannon, Acta Crystallogr. A32 (1976) 751.
[21] B. Markovsky, Y. Talyossef, G. Salitra, D. Aurbach, H.-J. Kim, S. Choi, Electrochem. Commun. 6 (2004) 821.
[22] J.C. Arrebola, A. Caballero, I. Hernán, J. Morales, Electrochem. Solid-State Lett. 8 (2005) A641.
[23] C. Sigala, A. Verbaere, J.L. Mansot, D. Guyomard, Y. Piffard, M. Tournoux, J. Solid State Chem. 132 (1997) 372.